

Communications

A Detector for a Chronic Implantable Atrial Tachyarrhythmia Monitor

Shantanu Sarkar*, David Ritscher, and Rahul Mehra

Abstract—Continuous long-term monitoring of atrial fibrillation (AF) and tachycardia (AT) is an unmet clinical need, which could be met with a chronically-implanted monitor. Improved therapeutic decisions based on accurate monitoring of parameters, such as daily AF/AT burden (hours/day) may lead to improvements in clinical outcomes such as reduction in hospitalizations, symptoms, and strokes. This paper describes an AF/AT detector that detects AF as well as AT with an irregular ventricular response, and a supplementary AT detector for AT with more regular ventricular response. Seven databases with significant durations of AF, AT, and sinus rhythm were used to evaluate the performance of the detectors. All patient records with AF ($N = 124$) were detected by the AF/AT detector to have AF/AT burden with a mean, median, and 75 percentile of absolute error in burden detection of 8.8, 0, and 4 min, respectively. In patients having AF burden (≥ 10 min), the AF/AT detector was found to have burden accuracy within 20% of true burden in 96% of patients. The specificity was 94%, defined as follows: in patient records without AF/AT ($N = 174$), the percentage with AF/AT burden ≤ 10 min in the 24-h recordings. The AF/AT detector underestimates AT burden, thus degrading performance, in patients with significant amounts of AT with more regular ventricular response. The supplementary AT detector reduces the underestimation of AT while overestimating burden in patients without a significant amount of AT. The detectors described here could be implemented in an implantable monitor for accurate long-term AF/AT monitoring.

Index Terms—Atrial fibrillation, atrial tachycardia, biomedical signal processing, implantable atrial tachyarrhythmia monitor, Lorenz plot.

I. INTRODUCTION

Atrial fibrillation (AF) and atrial tachycardia (AT) is prevalent in more than 2.2 million people in the United States, and will almost double in the next 20 years [1]. The goal of AF/AT management is to reduce the risk of stroke, by diagnosing AF/AT and initiating anticoagulation if other clinical risk factors exist, and improve clinical symptoms by reducing the amount of AF/AT the patients have (i.e., “rhythm control”), and by controlling the high ventricular rate due to AF/AT (i.e., “rate control”) [2]. The “snapshot” diagnostic techniques for AF/AT, such as an ECG examination, Holter monitoring, trans-telephonic-ECG, or event monitoring are inadequate. Although event monitoring improves the AF/AT diagnostic yield considerably, patient compliance limits this technique’s utility for continuous monitoring to much less than a month [3]. One key challenge with AF/AT monitoring is that the incidence of asymptomatic AF/AT can range between 20% and 50% [4], which may pose a high unperceived stroke risk in patients thought to be well rhythm controlled based on infrequent monitoring and symptoms. Continuous long-term monitoring of AF/AT burden may allow for evaluation of the true efficacy of pulmonary vein isolation [5] and anti-arrhythmic drug therapies [4], and

appropriate discontinuation of anticoagulation therapy in the absence of AF/AT to reduce the risk of bleeding during anticoagulation.

Chronic implantable monitors (CIM) with automatic AF/AT detection capabilities could be used for continuous long-term AF/AT monitoring in patients not indicated to receive a pacemaker or implantable cardioverter defibrillator (ICD). CIMs are implanted subcutaneously for automatic and patient triggered recording of ECG during cardiac events [6]. Unlike the pacemakers and ICDs, in which AF/AT is detected using a sensing lead inside the atrium, the CIM would need to detect AF/AT based on RR intervals, as the P wave amplitudes tend to be small. External monitoring devices have employed techniques to store automatically triggered AF/AT episodes in cardiac event recorders [3]. Various techniques for detecting AF, including the Lorenz plot of RR intervals, have been reported in literature [7]–[9]. None of these techniques will be able to detect AT, including atrial flutter, which does not have an irregular ventricular response. AT is as clinically relevant as AF with similar risk for strokes. This paper describes and evaluates the performance of an AF/AT detector that can provide daily monitoring of AF/AT over a long period of time and answer the key clinical questions regarding rhythm control such as the presence of AF/AT, and AF/AT burden (e.g., in hours per day) accurately. The detector uses the Lorenz distribution of a time series of RR intervals and is computationally simple for implementation in a CIM with limited processing power and constraints of maximizing battery life of the device.

II. METHODS

A. Detector Concepts and Design

Ventricular response during AF is controlled by conduction properties of the AV-node and is believed to be irregular and uncorrelated or “random” in nature [10]. AT can have very regular RR intervals due to consistent AV node conduction ratio (2:1, 3:1, etc.), irregular RR intervals like in AF, or regularly irregular ventricular response as a result of the mechanism called “group beating” [11]. An AF/AT detector, which detects based on irregularity of ventricular response, will detect AT with irregular ventricular response. A supplemental AT detector is required to detect AT with regularly irregular and regular ventricular response. The δRR interval, defined as $\delta RR(i) = RR(i) - RR(i-1)$, is a measure of irregularity. The Lorenz plot of δRR intervals, which is a scatter plot of $\delta RR(i-1)$ versus $\delta RR(i)$, encodes the uncorrelated nature of RR intervals in the direction of change of three consecutive RR intervals. Examples of 2 min of ECG during AF and AT along with the corresponding Lorenz plot of δRR intervals are shown in Fig. 1. The 2-D histogram shown in Fig. 2(a) is a numeric representation of a Lorenz plot extending from $[-\text{extent}, +\text{extent}]$ with bins of size binSize. Populating the 2-D histogram bins based on $\{\delta RR(i), \delta RR(i-1)\}$ values over a period of T minutes lead to characteristic signatures of a sequence of δRR intervals during AF/AT. The sequence of RR intervals that will populate the different segments in Fig. 2(a) is tabulated in Fig. 2(b). For example, segments 1 and 9 have an RR sequence of short interval followed by a long interval followed by a short interval (S–L–S). Segment 9 will be populated when $|\delta RR(i)| \cong |\delta RR(i-1)|$ while segment 1 will be populated when $|\delta RR(i)| \neq |\delta RR(i-1)|$. The width of segment 9, which is same as the width of segment 0 defined by parameter NSRmask, accounts for the variation due to autonomic modulation of the AV-node.

Manuscript received May 1, 2006; revised June 18, 2007. Asterisk indicates corresponding author.

*S. Sarkar is with Medtronic, Inc., 8200 Coral Sea Street NE, MVN41, Moundsview, MN 55112 USA (e-mail: shantanu.sarkar@medtronic.com).

D. Ritscher and R. Mehra are with the Cardiac Rhythm and Disease Management Research Division, Medtronic, Inc., Minneapolis, MN 55432 USA.

Digital Object Identifier 10.1109/TBME.2007.903707

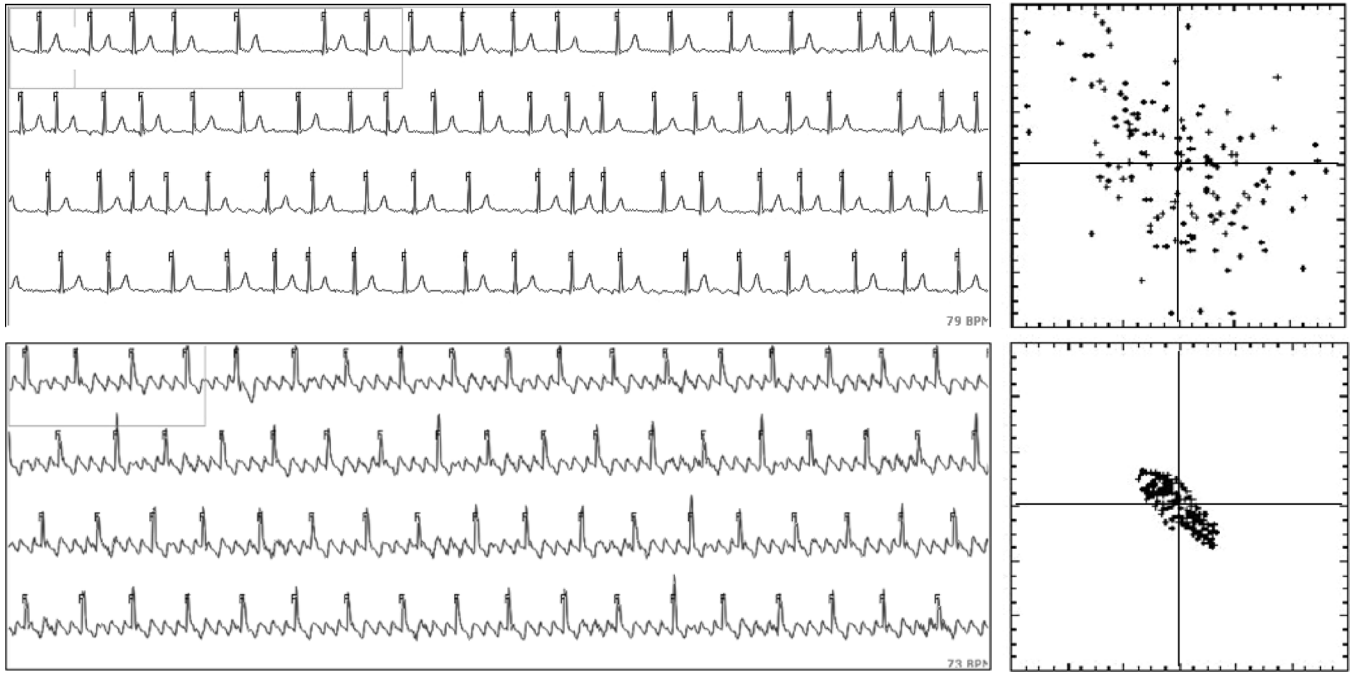


Fig. 1. Two example ECGs of 2 min in duration during atrial tachyarrhythmia and the corresponding patterns they map to in a Lorenz plot of δRR intervals. A 2-min strip of atrial fibrillation is shown in the first example, and a 2-min strip of atrial tachycardia is shown in the second example.

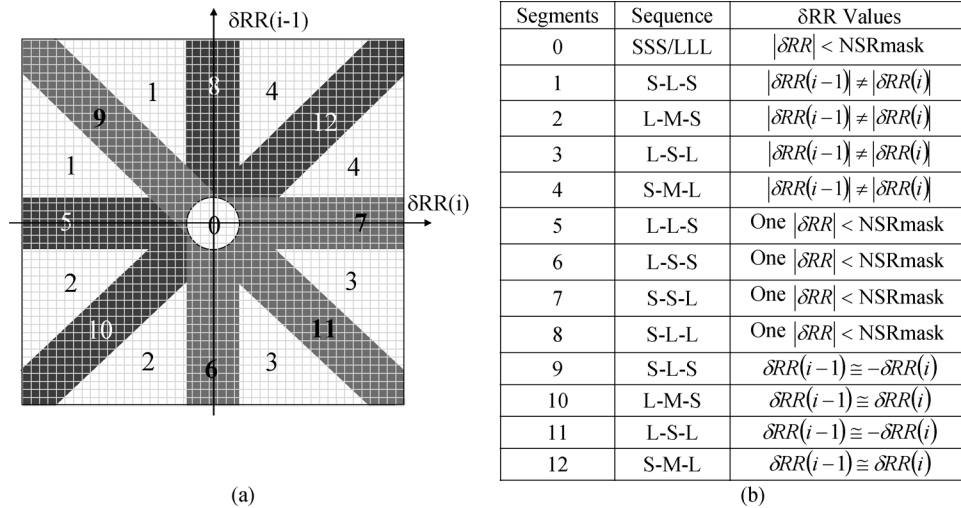


Fig. 2. (a) The 2-D histogram, a numeric representation of a Lorenz plot, of δRR intervals with the present δRR interval as the x axis variable and the previous δRR interval as the y axis variable. 13 segments are marked on the plot denoting regions that would be populated by $\{\delta RR(i), \delta RR(i-1)\}$ values for different sequences of RR intervals as tabulated in (b). An “S–M–L” sequence indicate a sequence of short RR interval followed by a longer (medium) interval followed by the longest interval. NSRmask is the radius of segment 0 and has a nominal value of 80 ms. The 2-D histogram was divided into segments 1–12 primarily for supplementary AT detection.

During normal sinus rhythm (NSR), bins within segment 0 of the 2-D histogram are mostly populated as shown in Fig. 3(a), whereas during AF, all segments are populated as shown in Fig. 3(f). The density of the distribution during AF varies with the underlying cycle length since the coefficient of variation of RR intervals is constant during AF [7], [8]. Fig. 3(b) shows the distribution during a series of premature atrial contractions leading to irregular RR intervals and exhibit specific distributions that are different than the AF/AT signatures. Fig. 3(c)–(e) shows different degrees of organization of ventricular response during AT with the most regular in (c), group beating in (d), and irregular like AF in (e). During AT, segments 0, 6, 7, 9, and 11 are populated most often.

The detector was developed by designing metrics that encoded the information regarding patterns in the 2-D histogram populated by

$\{\delta RR(i), \delta RR(i-1)\}$ values over a period of T minutes. IrregularityEvidence (1) measured the sparseness of the distribution with a high value during AF and a low value during NSR. DensityEvidence (2) measured the density in a cluster, and AnisotropyEvidence (3) measured the orientation of the distribution. The PACEvidence (4) measured the evidence of compensatory pauses.

$$\text{IrregularityEvidence} = \sum_{n=1}^{12} \text{BinCount}_n \quad (1)$$

$$\text{DensityEvidence} = \sum_{n=5}^{12} (\text{PointCount}_n - \text{BinCount}_n) \quad (2)$$

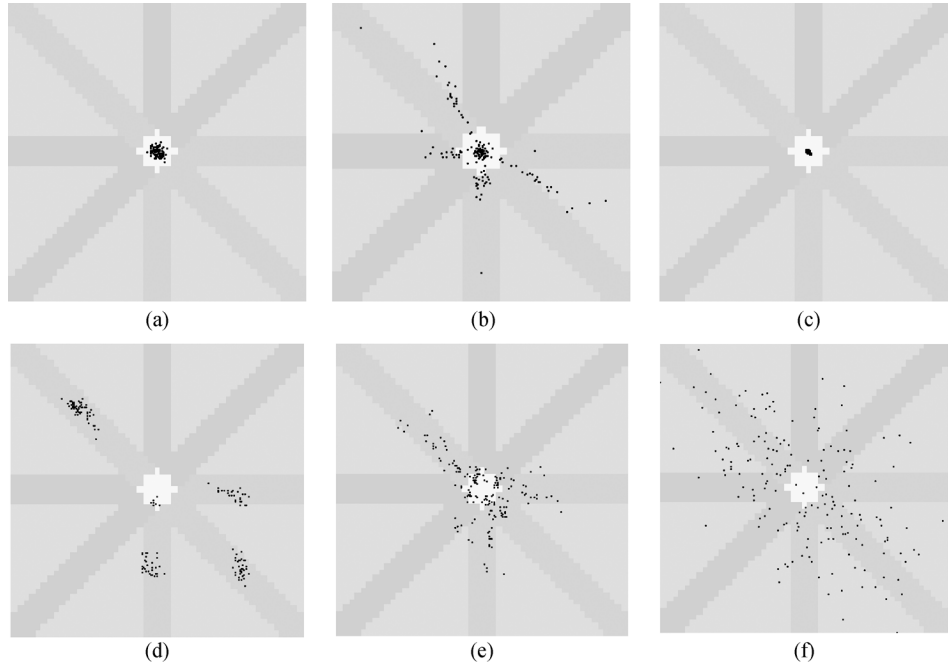


Fig. 3. Lorenz plot of δRR intervals overlaid on the segmented 2-D histogram for 2 min of data during (a) normal sinus rhythm, (b) series of premature atrial contractions, (c) atrial tachycardia (AT) with regular ventricular response, (d) AT with “group beating,” (e) AT with irregular ventricular response, and (f) atrial fibrillation. The plots exhibit various forms of irregularity in ventricular response. The Lorenz plots extended from -600 ms to $+600$ ms along both axes. The NSRmask value used for the underlying 2-D histogram was 80 ms.

AnisotropyEvidence

$$= \left| \sum_{n=9,11} \text{PointCount}_n - \sum_{n=10,12} \text{PointCount}_n \right| + \left| \sum_{n=6,7} \text{PointCount}_n - \sum_{n=5,8} \text{PointCount}_n \right| \quad (3)$$

PACEEvidence

$$= \sum_{n=1}^4 (\text{PointCount}_n - \text{BinCount}_n) + \sum_{n=5,6,10} (\text{PointCount}_n - \text{BinCount}_n) - \sum_{n=7,8,12} (\text{PointCount}_n - \text{BinCount}_n). \quad (4)$$

PointCount_n counted the number times bins in segment n were populated. BinCount_n counted the number of bins in segment n of the histogram that were populated at least once. AFEvidence, ATEvidence, and OrgIndex metrics (5)–(7) were computed using (1)–(4), OriginCount, and Regularity Evidence.

$$\text{AFEvidence} = \text{IrregularityEvidence} - \text{OriginCount} - 2 * \text{PACEEvidence} \quad (5)$$

$$\text{ATEvidence} = \text{IrregularityEvidence} + \text{AnisotropyEvidence} + \text{DensityEvidence} + \text{RegularityEvidence} - 4 * \text{PACEEvidence} \quad (6)$$

$$\text{OrgIndex} = \text{OriginCount} + \text{AnisotropyEvidence} + \text{DensityEvidence} + \text{RegularityEvidence} - 2 * \text{IrregularityEvidence}. \quad (7)$$

OriginCount is the count of the number of $\{\delta RR(i), \delta RR(i-1)\}$ values in the bin containing the origin. RegularityEvidence was computed as the number of short term medians that were not different than

the long term median of RR intervals in the previous T minute period by more than 10 ms. Short-term medians, for the previous 6 or 12 beats, were computed every multiple of the sixth beat or twelfth beat from the start of the present T minute period.

The detector operates in the base “AF/AT mode,” which detects AF and AT with irregular ventricular response, by comparing AFEvidence to AFThreshold to detect AF. In the “supplemental AT mode,” AF is detected if AFEvidence \geq AFThreshold and ATEvidence $<$ ATThreshold. AT is detected if ATEvidence \geq ATThreshold and AFEvidence $<$ AFThreshold or if RegularityEvidence \geq RegularityThreshold. If AFEvidence \geq AFThreshold and ATEvidence \geq ATThreshold then AF is detected if OrgIndex $<$ 0 else AT is detected. Two patent applications are pending [12] and one has been issued [13] relating to these detectors.

B. Databases

Seven long-term Holter databases were used to test the detector. Three MIT-BIH databases [14], MIT-BIH AF database (25 patients, 92 h of AF, 144 h of NSR), MIT-BIH NSR database (18 patients, 384 h of NSR), MIT-BIH NSR RR Interval database (54 patients, 1276 h of NSR), were used. An “AF database” (81 patients, 476 h of AF, 76 h of AT, 1397 hours of NSR) was compiled such that onset of AF were clearly visible in the Holter recordings. An “AT database” (124 patients, 20 h of AF, 2000 h of AT, 915 h of NSR) was compiled of Holter recordings of AT (primarily atrial flutter) for developing the supplemental AT detector. The “NSR database” (102 patients, 2418 h of NSR) was compiled by selecting 100 consecutive patients who were prescribed a Holter recording, and were predominantly in NSR. Patients with AF (4) were shifted to the AF database. The “Chronic AF” database (18 patients, 422 h of AF) consisted of Holter recordings of patients in AF. All database annotations were performed by the database providers. Five records from the MIT-BIH AF database, ten files from the AF database, and 20 records from the AT database were used to develop the AF/AT detector and the supplemental AT detector. These

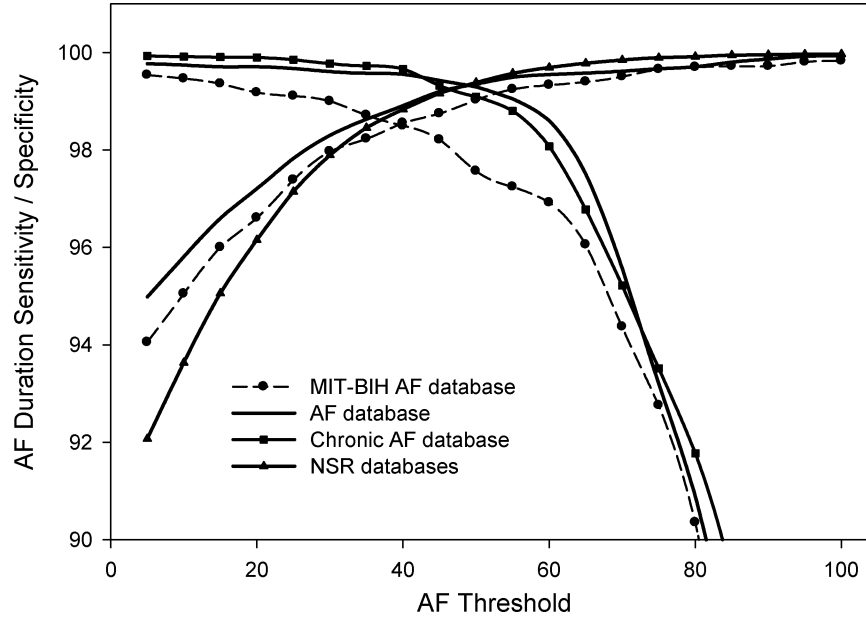


Fig. 4. Duration sensitivity and specificity curves for the AF/AT detector with respect to the AF threshold for AF and NSR databases. Duration sensitivity reduces while duration specificity increases with increase in threshold. The chronic AF and NSR databases only have sensitivity and specificity curves respectively.

records were selected to represent the varying degree of ventricular response during AF/AT, ranging from patients with paroxysmal episodes to patients with > 24 h episodes.

C. Detector Optimization

The detector results for every T minute period were compared to the annotations to evaluate the performance of the detector [15] with a conversion of annotations to T -minute resolution. If more than 60% of the intervals within the T minutes were AF or AT then the annotation was AF or AT for that T -minute period. The value of 60% was chosen empirically to ensure that in a T -minute period with AF/AT onset or termination, close to half of the period and close to half of δ RR values that populated the histogram were during AF/AT. True positives (TP), true negatives (TN), false positives (FP) and false negatives (FN) were computed for each record and then added for all records to compute the overall performance metrics for databases or combinations. Parameter optimization and a technical evaluation of the algorithm was performed using the duration sensitivity, $DS_n = TP / (TP + FN)$ and duration specificity, $DS_p = TP / (TP + FP)$ metrics that are surrogate measures of burden. DS_n and DS_p evaluate the ability of the detector to measure true arrhythmia duration and reject non-arrhythmia periods, respectively.

D. Performance Evaluation of Burden

An accurate measure of AF/AT burden will answer the primary diagnostic question to determine whether a patient has any AF/AT and the monitoring question to accurately quantify the amount of AF/AT. Detection sensitivity (percent of records with detected burden amongst records with true burden), detection specificity (percent of records with detected burden < 10 min. amongst records with no burden), statistics of absolute error in burden, and relative error (percent records with detected burden within 10% and 20% of the true burden) was reported to evaluate burden accuracy.

E. Episode Detection Performance

The episode detection sensitivity (ES_n : ability to detect a true AF/AT episode) and PPV (% of detected episodes having true AF/AT) metrics [15] were evaluated at thresholds chosen for optimal burden accu-

racy. Since the detector was designed to decide every 2 min, only true episodes > 2 min in duration were considered.

F. Validation of Detector

Validation was performed using the bootstrap technique as it offers the additional benefit of providing a performance bound. Due to the large number of datasets and the statistical nature of the detector, development database bias was minimal. All 298 patients from the AF, MIT-BIH AF, and all the NSR databases were used to create the "AF+NSR" dataset to evaluate the performance of the AF/AT detector. The bootstrap procedure had been defined to select, without replacement, 100 random patients from the "AF+NSR" dataset and computed the DS_n and DS_p metrics. To create an "AT+AF+NSR" dataset for evaluating the performance of the supplemental AT detector, 25 patients were randomly chosen from the AT database and added to the 100 randomly chosen records from the "AF+NSR" dataset. The selections were repeated 100 000 times to obtain the performance bounds.

III. RESULTS

1) *Detector Optimization*: The parameters were optimized for the detector's ability to detect AF duration (hence AF burden) accurately using the AF database. The optimal parameters were $T = 2$ min, $\text{binSize} = 40$ ms, $\text{extent} = 600$ ms, $\text{NSRmask} = 80$ ms, and $\text{AF Threshold} = 50$. The parameter values were selected based on area under the ROC curve using DS_n and DS_p with constraints of memory and computational requirements. The DS_n and DS_p curves for the AF/AT detector using the default parameters are shown in Fig. 4. At the optimal AF Threshold of 50, DS_n was 99.3%, 97.5%, and 98.5% for the AF, MIT-BIH AF, and chronic AF databases, respectively. DS_p was 99.4%, 99.0%, and 99.4% for AF, MIT-BIH AF, and all NSR databases respectively. DS_n was 57.7% and DS_p was 98.8% in the AT database.

DS_n and DS_p values of 92% was obtained with the supplemental AT detector for an AT Threshold of 110 and $\text{Regularity Threshold}$ of 94 in the AT database. The amount of AF will be much higher than AT, hence thresholds were selected to obtain $DS_p > 95\%$. An AT Threshold of 160 and $\text{Regularity Threshold}$ of 100 was chosen, resulting in a DS_p of 95.8%, 97.0%, 97.6%, and 90.4% in the AT, AF, combined NSR, and

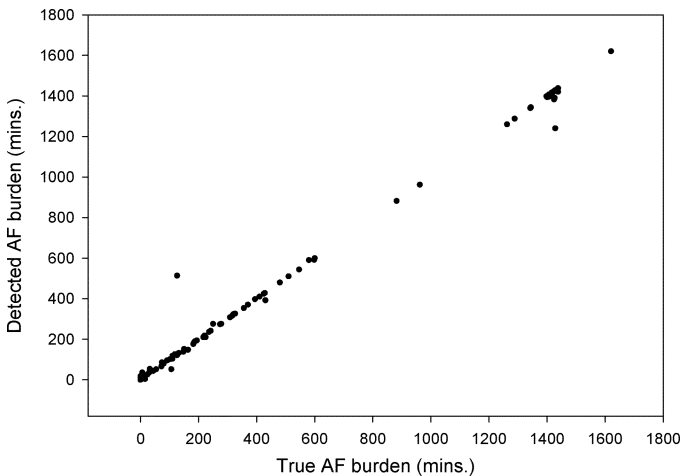


Fig. 5. Detected versus true AF burden using the AF/AT detector in 124 patient records from the AF, MIT-BIH AF, and chronic AF databases. Points below the unity line represent underestimation of burden.

MIT-BIH AF databases, respectively. The DS_n was 82.2% for the AT database and improved marginally over the AF/AT detector results in other databases.

A. Performance Evaluation of the AF/AT Detector

1) *AF/AT Burden*: Fig. 5 compares the detected AF/AT burden with true AF burden for MIT-BIH AF, chronic AF, and AF databases. For the 124 patient records the mean, median, and 75 percentile of absolute error in burden detection was 8.8, 0, and 4 min, respectively. The detection sensitivity was 100% (all 100 patient records which had true AF burden had detected AF burden). For the 90 patient records with AF (≥ 10 min), 90%, and 96% had detected AF burden within 10%, and 20% of true AF burden, respectively. For a combination of patient records such that there is 90% AF burden and 10% AT burden (16 randomly selected patients from AT database for a total of 140 patients), detection sensitivity was 100%. Of records with AF/AT (≥ 10 min), 87% and 92% had detected burden within 10% and 20% of true burden, respectively. The mean, 25 percentile, median, and 75 percentile of absolute error were 35, 0, 2, and 6 min, respectively. The 16 AT patients in this cohort contributed to 28 of the 35 min of mean error. Detection specificity was 94% (detected AF/AT burden ≤ 10 min in 163 out of 174 patient records in NSR databases) with a mean and 75 percentile of absolute error of 3.6 and 0 min, respectively.

2) *AF Episodes*: The ES_n and PPV was 94.7% and 95.8%, respectively, in the MIT-BIH AF database and 96.4% and 79.4%, respectively, in the AF database for AF threshold of 50 which is optimal for burden detection. ES_n and PPV was 94.4% and 93.9%, respectively, at an AF threshold of 65 for the AF database. For the NSR databases there were 238 false episode detections (100 episodes 2 min in duration and 21 episodes > 10 min in duration) in 27 of 174 patient records with 4 records contributing to 135 of these false detections. Due to the short duration of the false detections, burden metric is minimally affected.

3) *Validation and Performance Bounds*: The bootstrap validation of the AF/AT detector performed using the “AF+NSR” data set showed a mean, 5th percentile, and lowest value of 99.0%, 98.0%, and 95.0%, respectively, for DS_n and 99.5%, 99.0%, and 98.0%, respectively, for DS_p . For the “AT+AF+NSR” dataset the AF/AT detector had a mean, fifth percentile, and lowest DS_n of 80.3%, 68.0%, and 48.4%, respectively, with similar statistics for DS_p as mentioned above. The AF/AT detector operates very accurately in detecting AF duration, but performance reduces in presence of significant amount of AT.

B. Incremental Impact of the Supplementary at Detector

Underestimation of AT burden was reduced in 2% of patients in the cohort of 140 patients (with 90% AF burden and 10% AT burden) using the supplemental AT detector; however, due to overestimation of burden in patients with low AF/AT burden, % records with AF/AT (≥ 10 min) with detected burden within 10% and 20% of true burden reduced by 14% and 3%, respectively. The mean error reduced by 69% in the 16 patients randomly selected from AT database to form the cohort; however detection specificity reduced by 18%. The overestimation degrades overall performance if the patient population has very little AT. An improvement in sensitivity over the AF/AT detector was obtained if the %AT burden exceeded 40% in the cohort. The validation using the AT, AF, and NSR dataset showed that DS_n improved from 80.3% to 92.1% and the DS_p reduced from 99.5% to 96.7%.

IV. DISCUSSION

Continuous long-term AF burden measure will enable accurate evaluation of “rhythm control” particularly in patients with asymptomatic and paroxysmal AF/AT. Efficacy of “rate control” therapies can be measured accurately by evaluating the ventricular rate for the entire duration of AF. The detector presented in this paper is computationally simple enough to be implemented in a chronic implantable monitor (CIM) that can provide daily rhythm control and rate control diagnostic information in AF patients over a long period of time and provide supplemental AT detection capabilities.

The detectors were optimized with respect to the AF duration, which is a surrogate of AF burden. The AF/AT detector was found to be accurate in measuring AF burden. The AF/AT detector performance degrades if there is a significant amount of AT burden in the patient population. Detection of paroxysmal AF, specifically isolated episodes < 2 min in duration, was affected due to the lack of synchronization of the 2-min detection periods with the onset or termination of AF/AT episodes. The detector performs better for episodes that are longer than 3 min, which ensures 75% of a 2-min period with AF/AT. The use of a fixed time period of 2 min will bias the detector in performing better for faster ventricular rates as more evidence is accumulated in a 2-min period with larger number of RR intervals.

The supplemental AT detection capabilities in the detector can be useful in patients with a lot of AT, particularly with a more regular ventricular response, as well as in cases where sensitivity to all arrhythmias is more important than specificity. Incorporation of the AT detector improves the ability to detect AT, however the burden detection specificity is compromised. More than half of the loss in specificity resulted from the regularity criterion of the supplemental AT detector, particularly in patients with compromised autonomic tone and reduced heart rate variability, e.g., patients with heart failure. The regularity criteria in the supplemental AT detector should be turned off in such patients. It is important to study the AF as well as the supplemental AT detector prospectively in a clinical setting.

A. Limitations

Performance was evaluated using a retrospective analysis on available databases with up to 24-h-long records. Although effort was made to include adequate numbers of non-arrhythmia records, the performance is clearly a function of the databases used. The database annotations for cardiac rhythm were done by experts but have a component of subjectivity, especially when differentiating between AF or AT. The detector’s performance will depend on the fidelity of RR intervals.

REFERENCES

- [1] T. Thom *et al.*, “Heart disease and stroke statistics-2006 update,” *Circulation*, vol. 113, pp. e85–151, 2006.

- [2] V. Fuster *et al.*, "ACC/AHA/ESC guidelines for the management of patients with atrial fibrillation," *Eur. Heart J.*, vol. 22, pp. 1852–923, 2001.
- [3] C. R. Vasamreddy, D. Dalal, J. Dong, A. Cheng, D. Spragg, S. Z. Lami, G. Meininger, C. A. Henrikson, J. E. Marine, R. Berger, and H. Calkins, "Symptomatic and asymptomatic atrial fibrillation in patients undergoing radiofrequency catheter ablation," *J. Cardiovasc. Electrophysiol.*, vol. 17, pp. 134–9, 2006.
- [4] C. W. Israel, G. Gronefeld, J. R. Ehrlich, Y. G. Li, and S. H. Hohnloser, "Long-term risk of recurrent atrial fibrillation as documented by an implantable monitoring device: Implications for optimal patient care," *J. Amer. Coll. Cardiol.*, vol. 43, pp. 47–52, 2004.
- [5] H. Purerfellner, J. Aichinger, M. Martinek, H. J. Nesser, P. Ziegler, J. Koehler, E. Warman, and D. Hettrick, "Quantification of atrial tachyarrhythmia burden with an implantable pacemaker before and after pulmonary vein isolation," *Pacing Clin. Electrophysiol.*, vol. 27, pp. 1277–83, 2004.
- [6] K. Seidl, M. Rameken, S. Breunung, J. Senges, W. Jung, D. Andresen, A. van Toor, A. D. Krahn, and G. J. Klein, "Diagnostic assessment of recurrent unexplained syncope with a new subcutaneously implantable loop recorder. Reveal-investigators," *Europace*, vol. 2, pp. 256–62, 2000.
- [7] T. Anan, K. Sunagawa, H. Araki, and M. Nakamura, "Arrhythmia analysis by successive RR plotting," *J. Electrocardiol.*, vol. 23, pp. 243–8, 1990.
- [8] K. Tateno and L. Glass, "Automatic detection of atrial fibrillation using the coefficient of variation and density histograms of RR and deltaRR intervals," *Med. Biol. Eng. Comput.*, vol. 39, pp. 664–71, 2001.
- [9] D. Duverney, J. M. Gaspoz, V. Pichot, F. Roche, R. Brion, A. Antoniadis, and J. C. Barthelemy, "High accuracy of automatic detection of atrial fibrillation using wavelet transform of heart rate intervals," *Pacing Clin. Electrophysiol.*, vol. 25, pp. 457–62, 2002.
- [10] B. K. Bootsma, A. J. Hoelsen, J. Strackee, and F. L. Meijler, "Analysis of R-R intervals in patients with atrial fibrillation at rest and during exercise," *Circulation*, vol. 41, pp. 783–94, 1970.
- [11] M. Duytschaever, C. Dierickx, and R. Tavernier, "Variable atrioventricular block during atrial flutter: What is the mechanism?," *J. Cardiovasc. Electrophysiol.*, vol. 13, pp. 950–1, 2002.
- [12] S. Sarkar and D. Ritscher, "Method and apparatus for detection of tachyarrhythmia using cycle lengths," U.S. Patent Application 200 602 247 547 A1, Nov. 2, 2006.
- [13] D. Ritscher and S. Sarkar, "Algorithms for detecting atrial arrhythmias from discriminatory signatures of ventricular cycle lengths," U.S. Patent 7 031 765 B2, Apr. 18, 2006.
- [14] A. L. Goldberger, L. A. Amaral, L. Glass, J. M. Hausdorff, P. C. Ivanov, R. G. Mark, J. E. Mietus, G. B. Moody, C. K. Peng, and H. E. Stanley, "PhysioBank, PhysioToolkit, and PhysioNet: Components of a new research resource for complex physiologic signals," *Circulation*, vol. 101, pp. E215–20, 2000.
- [15] "Testing and reporting performance results of cardiac rhythm and ST segment measurement algorithms," ANSI/AAMI EC57, 1998 [Online]. Available: http://www.accessdata.fda.gov/scripts/cdrh/cfdocs/cfStandards/Detail.CFM?STANDARD_IDENTIFICATION_NO=8510

A Quantitative Method Based on Total Relative Change for Dynamic Electrical Impedance Tomography

Fusheng You, Xuetao Shi, Xiuzhen Dong*, *Member, IEEE*,
Feng Fu, Ruigang Liu, Wanjun Shuai, and Zheng Li

Abstract—We proposed a new method based on total relative change (TRC) from measured boundary voltages to quantify the volume changes of fluid during electrical impedance tomography (EIT) monitoring. The results showed that TRC linearly correlated with the volume of infused saline solution into a phantom, and the slope of TRC changes was approximately linear with the infusion speed. A inserted copper tube at different positions did not affect TRC significantly. The linear relationship between TRC and volume change indicates that TRC could be a good quantitative index for dynamic EIT.

Index Terms—Electrical impedance tomography, quantification, total relative change.

I. INTRODUCTION

DYNAMIC electrical impedance tomography (EIT) is a non-ionizing method and can be applied continuously for long-term patient monitoring [1], [2]. It is essential to quantify the volume changes of air or fluid inside the body during the monitoring. The resistivity index (RI) is currently used as a quantitative index for fluid or air changes. Studies have shown an approximate linear relationship between RI and the volume changes [3]–[5]. Such consistent linear relationship has also been found between RI and the volume of solutions added to the peritoneum in continuous ambulatory peritoneal dialysis (CAPD) patients [6] and between RI and lung volume during monitoring the function of lung ventilation [7], [8].

The reported RI is the summation of all resistivity values in a given region of interesting (ROI) in the reconstructed image. In this study we analyzed the measurement data and proposed a new quantitative method based on the total relative change (TRC) of the measurement data.

II. MATERIALS AND METHODS

A. Hardware System and Phantom

The EIT system (FMMU V3.5) with 32 silver compound-electrodes [9] was used in this study. The phantom consisted of a cylindrical tank with 10 cm in height and 30 cm in diameter. The tank was filled with 4000 mL 0.125% NaCl solution as background and the electrodes were attached to the tank boundary.

B. Calculation of Total Relative Change

The TRC is calculated by adding up all the relative changes (RC) according to the following equation:

$$TRC = \sum_{i=1}^{N_1} \sum_{j=1}^{N_2} RC(i, j) = \sum_{i=1}^{N_1} \sum_{j=1}^{N_2} \frac{D_2(i, j) - D_1(i, j)}{D_1(i, j)}; \quad i = 1, 2, \dots, N_1; \quad j = 1, 2, \dots, N_2 \quad (1)$$

Manuscript received November 22, 2006; revised May 21, 2007. This work was supported in part by the Key Project of Natural Science Foundation of China under Grant 50337020. Asterisk indicates corresponding author.

F. You, X. Shi, F. Fu, R. Liu, W. Shuai, and Z. Li are with the Department of Biomedical Engineering, Fourth Military Medical University, Xi'an 710032, China. (e-mail: yfusheng@263.net)

*X. Dong is with the Department of Biomedical Engineering, Fourth Military Medical University, ChangLe West Street 17#, Xi'an 710032, China (e-mail: dongxiuzhen@fmmu.edu.cn)

Digital Object Identifier 10.1109/TBME.2007.905487